JOURNAL OF MATERIALS SCIENCE **39** (2004) 193–200

Cu^{2+} ions in sodium fluoride-sodium borate glasses studied by EPR and optical absorption techniques

P. G. PRAKASH, J. L. RAO
Department of Physics, Sri Venkateswara University, Tirupati-517 502, India
E-mail: jlrao46@yahoo.co.in

Electron paramagnetic resonance (EPR) and optical absorption spectra of Cu^{2+} ions in $80Na_2B_4O_7$-$(20 - x)$NaF $- x$CuO (NFNB) glass system with $0 \leq x \leq 6$ mol% have been studied. EPR spectra of all the glass samples exhibit resonance signals characteristic of Cu^{2+} ions. The values of spin-Hamiltonian parameters indicate that the Cu^{2+} ions in sodium fluoride-sodium borate (NFNB) glasses were present in octahedral sites with tetragonal distortion. The number of spins (N) participating in resonance was calculated as a function of temperature for NFNB glass sample containing 1 mol% of Cu^{2+} ions and the activation energy was calculated. From the EPR data, the paramagnetic susceptibility (χ) was calculated at various temperatures and the Curie constant was calculated from the $1/\chi - T$ graph. The optical absorption spectra of these samples show a broad absorption band centered at 13280 cm^{-1} which is assigned to the $^2B_{1g} \rightarrow {}^2B_{2g}$ transition of Cu^{2+} ions in distorted octahedral sites. The optical band gap energy (E_{opt}) and Urbach energy (ΔE) are calculated from their ultraviolet edges. It is observed that as the copper ion concentration increases, E_{opt} decreases while ΔE increases. This has been explained as due to the creation of additional localized states by CuO, which overlap and extend in the mobility gap of the matrix. By correlating the EPR and optical data, the molecular orbital coefficients have been evaluated.

1. Introduction

The structure and properties of oxide glasses containing fluorine ions are important because of their potential application in IR fiber optics, laser windows and multifunctional optical components [1]. Moreover, the spectroscopic studies have shown that these glasses can be considered as promising candidates for electrochemical applications [2], such as power sources, especially in the field of solid state batteries.

Alkali haloborate glasses find applications as fast ionic conductors [3–5] with most of research work centered on lithium chloroborate system. Among other haloborate glasses, sodium fluoroborate has been of much interest for several research workers [3, 4, 6]. Measurements of glass forming behaviour, density, refractive index, viscosity, thermal expansion, glass transformation temperature and electrical conductivity have been reported [6] on sodium fluoroborate and NaF-Na_2O-B_2O_3 glasses.

Electron paramagnetic resonance (EPR) has been successfully applied to get information about transition metal ions in various glass systems. The ability to characterize the local structure of a paramagnetic center and sensitive detection of structural changes form the basis for the increasing number of applications of the EPR technique to glasses. Studies of EPR and optical properties of transition metal ions in glasses have made it possible not only to interpret the energy levels involved in the observed transitions, but also to comment on the chemical and structural environments about the metal ion center. This paper describes EPR and optical absorption studies of Cu^{2+} ions in the sodium fluoride-sodium borate glass system (hereafter to be referred as NFNB glass system).

2. Experimental techniques

The glass samples were prepared by the melt quenching method with the compositions given in Table I. The starting materials (analar grade s.d. fine chemicals with 99.5% purity) used in the present work were NaF, $Na_2B_4O_7 \cdot 10H_2O$ and CuO. All the chemicals were weighed accurately using an electrical balance, ground to fine powder and mixed thoroughly. The batches were melted at 850°C in porcelain crucibles by placing them in an electrical furnace. The melts were then poured on a polished brass plate and pressed quickly with another brass plate. The glasses thus obtained were transparent and bluish in colour. Care was taken to obtain glasses of uniform thickness for recording optical absorption spectra. Good quality glasses obtained after polishing were used for optical measurements.

The room temperature Electron Paramagnetic Resonance spectra of sodium fluoride–sodium borate

TABLE I Composition (mol%) and calculated optical basicities of the glasses studied in the present work

Glass system	Glass code	$Na_2B_4O_7$	NaF	CuO	Optical basicity (Λ_{th})
Sodium fluoride-Sodium borate	NFNB	80	20	–	0.5197
Sodium fluoride-Sodium borate:0.25CuO	NFNB0.25Cu	80	19.75	0.25	0.5184
Sodium fluoride-Sodium borate:0.5CuO	NFNB0.5Cu	80	19.50	0.50	0.5181
Sodium fluoride-Sodium borate:1CuO	NFNB1Cu	80	19	1	0.5172
Sodium fluoride-Sodium borate:2CuO	NFNB2Cu	80	18	2	0.5168
Sodium fluoride-Sodium borate:4CuO	NFNB4Cu	80	16	4	0.5153
Sodium fluoride-Sodium borate:6CuO	NFNB6Cu	80	14	6	0.5145

(NFNB) glasses containing different mol% of Cu^{2+} ions were recorded on an EPR spectrometer (JEOL FEIX) operating in the X-band frequencies (9.205 GHz) with a modulation frequency of 100 kHz. The magnetic field was scanned from 220 to 420 mT with a scan speed of 25 mT min^{-1}. A powdered glass specimen of 100 mg was taken in a quartz tube for EPR measurements. Polycrystalline Di-Phenyl Picryl Hydrazyl (DPPH) with a g value of 2.0036 was used as a standard field marker. The EPR spectrum of the $CuSO_4{\cdot}5H_2O$ powdered substance was also recorded as a reference to calculate the number of spins.

The EPR spectrum of 1 mol% CuO doped NFNB glass sample was recorded at different temperatures (163–393 K) using a variable temperature controller (JES UCT 2AX). A temperature stability of ± 1 K was easily obtained by waiting approximately half an hour at the set temperature before recording a spectrum, at each temperature.

Optical absorption spectra of NFNB, NFNB0.5Cu, NFNB1Cu samples doped with copper ions were recorded at room temperature on a JASCO-V570 UV-VIS-NIR spectrophotometer in the wavelength region λ 250 to 1300 nm. Glass samples of thickness 1 mm were used for optical measurements.

3. Results and analysis

3.1. EPR studies

No EPR signal is observed in undoped glasses confirming that the starting materials used in the present work were free from transition metal impurities or other paramagnetic centres (defects). When Cu^{2+} ions were added to the NFNB glasses, the EPR spectra exhibit resonance signals similar to those reported for Cu^{2+} ions in Na_2O-P_2O_5, K_2O-B_2O_3, K_2SO_4-$ZnSO_4$ glasses [7], Soda-borate glasses [8] and $R_2B_4O_7$-PbO-TeO_2 (R = Li, Na or K) glasses [9]. The Cu^{2+} ion with $S = 1/2$ has a nuclear spin $I = 3/2$ for both ^{69}Cu (the natural abundance 69%) and ^{65}Cu (natural abundance 31%) and therefore $(2I + 1)$ i.e., four parallel and four perpendicular hyperfine (hf) components would be expected. In the recorded spectra, we observed three weak parallel components in the lower field region and the fourth parallel component is overlapped by the perpendicular component. The perpendicular components in the high field region are well resolved. The EPR spectra of different concentrations (mol%) of Cu^{2+} ions doped in NFNB glass system at room temperature are shown in Fig. 1.

The number of spins participating in resonance can be calculated by comparing the area under the absorption curve with that of a standard ($CuSO_4{\cdot}5H_2O$) of known concentration. Weil *et al.* [10] gave the following expression, which includes the experimental parameters of both sample and standard.

$$N = \frac{A_x(\mathrm{Scan_x})^2\, G_{std}(B_m)_{std}(g_{std})^2[S(S+1)]_{std}(P_{std})^{1/2}}{A_{std}(\mathrm{Scan_{std}})^2\, G_x(B_m)_x(g_x)^2\,[S(S+1)]_x(P_x)^{1/2}}[\mathrm{Std}] \tag{1}$$

where 'A' is the area under the absorption curve which can be obtained by double integrating the first derivative absorption curve; 'Scan' is the magnetic field corresponding to the unit length of the chart; 'G' is the gain; 'B_m' is the modulation field width, 'g' is the g factor; 'S' is the spin of the system in its ground state and 'P' is the power of the microwaves applied. The subscripts 'x' and 'std' represent the corresponding quantities for Cu^{2+} glass sample and the reference ($CuSO_4{\cdot}5H_2O$) respectively.

The number of spins participating in resonance in this glass system was calculated for different concentrations ($0 \leq x \leq 6$ mol%). Fig. 2 shows a plot between number of spins and copper concentration for this glass system.

Fig. 3 shows the EPR spectra of NFNB1Cu glass sample recorded at different temperatures. The number of spins participated in the resonance was calculated at various temperatures and a plot was drawn between log N and $1/T$ for this sample and is shown in Fig. 4.

3.2. Calculation of susceptibility from EPR data

The paramagnetic susceptibility can be calculated from the EPR data using the formula

$$\chi = \frac{Ng^2\beta^2 J(J+1)}{3k_B(T)} \tag{2}$$

where N is the number of spins/kg and the rest of the symbols have their usual meaning. N can be calculated using Equation 1 and $g[=(g_\parallel + 2g_\perp)/3]$ is taken from EPR data. The paramagnetic susceptibilities were calculated for NFNB1Cu glass sample at various temperatures. A plot of the reciprocal of susceptibility ($1/\chi$) as a function of absolute temperature (T) is shown in Fig. 5.

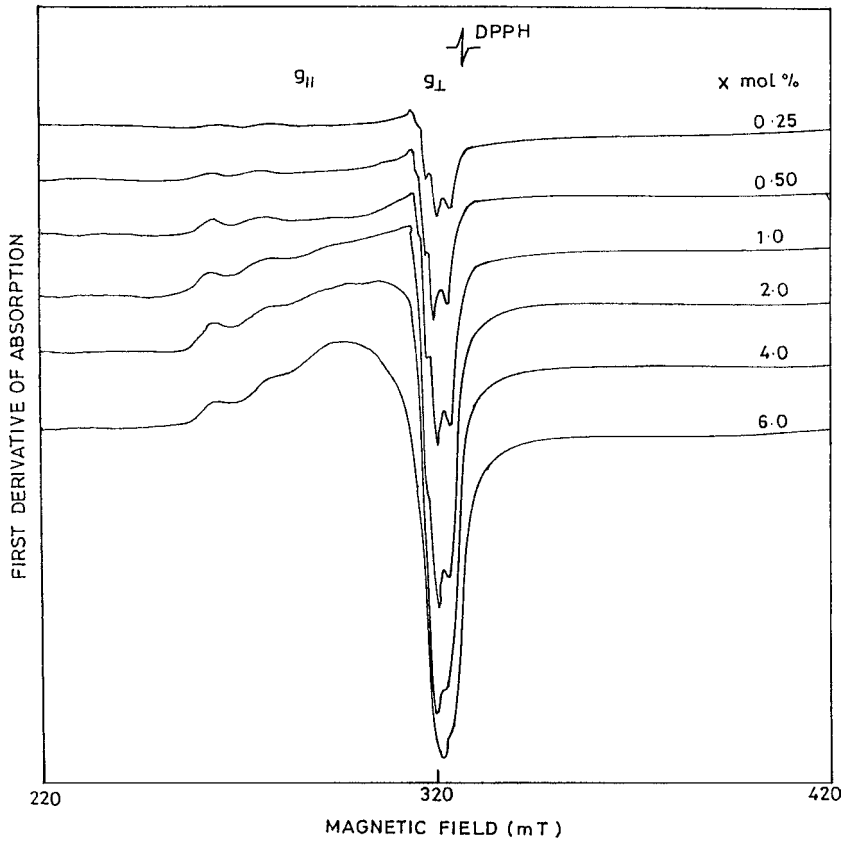

Figure 1 EPR spectra of different mol% of Cu^{2+} ions doped in sodium fluoride-sodium borate glass system at room temperature.

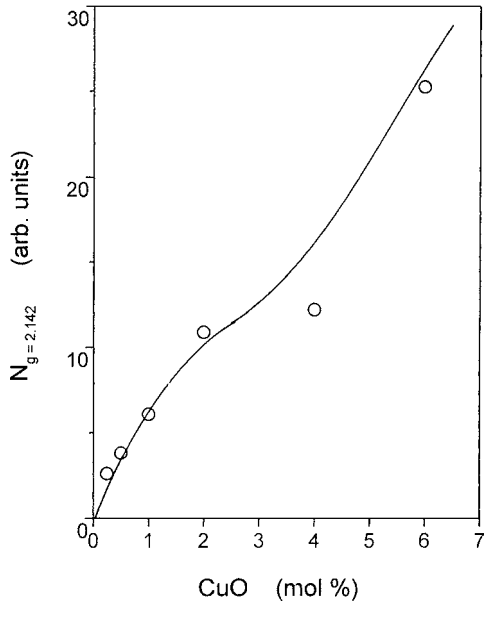

Figure 2 Variation of number of spins with mol% of Cu^{2+} ions doped in sodium fluoride-sodium borate glass system at room temperature.

3.3. Optical absorption spectrum

Fig. 6 shows the optical absorption spectrum of NFNB0.5Cu glass sample at room temperature observed between 500 nm and 1300 nm. From the figure, we can observe single broad band centred at 756 nm (13280 cm^{-1}). The optical absorption spectra of other samples are very similar to Fig. 6 showing single broad band corresponding to the transition $^2B_{1g} \rightarrow {}^2B_{2g}$. Similar results were reported in literature [11–14].

3.4. Optical band gap energy (E_{opt}) and Urbach energy (ΔE)

A main feature of the absorption edge of amorphous semiconductors, particularly at the lower values of absorption coefficient, is an exponential increase of the absorption coefficient $\alpha(\nu)$ with photon energy $h\nu$ in accordance with an empirical relation [15]

$$\alpha = \alpha_0 \exp(h\nu/\Delta E) \tag{3}$$

where 'α_0' is a constant, 'ΔE' is the Urbach energy which indicates the width of the band tails of the localized states and 'ν' is the frequency of radiation. The broadening of the exciton levels at the absorption edge is dominated by random electric fields due to either the lack of long-range order or the presence of defects [16, 17].

For an absorption by indirect transitions, the equation takes the form

$$E_{opt} = h\nu - (\alpha h\nu/A)^{1/2} \tag{4}$$

where 'A' is a constant and E_{opt} is the optical band gap energy. This relation applies to many oxide glasses [15]. Plots were drawn between $(\alpha h\nu)^{1/2}$ and $h\nu$. Fig. 7a and b show the ultraviolet absorption edge and corresponding $(\alpha h\nu)^{1/2}$ vs. $h\nu$ graph for NFNB, NFNB0.5Cu and NFNB1Cu glass samples. The optical band gap is obtained by extrapolating the linear region of the curve to the $h\nu$ axis. For these glass samples, plots were also drawn between $\ln\alpha$ and $h\nu$ as shown in Fig. 7c. From these plots, the slopes and thereby Urbach energies were calculated.

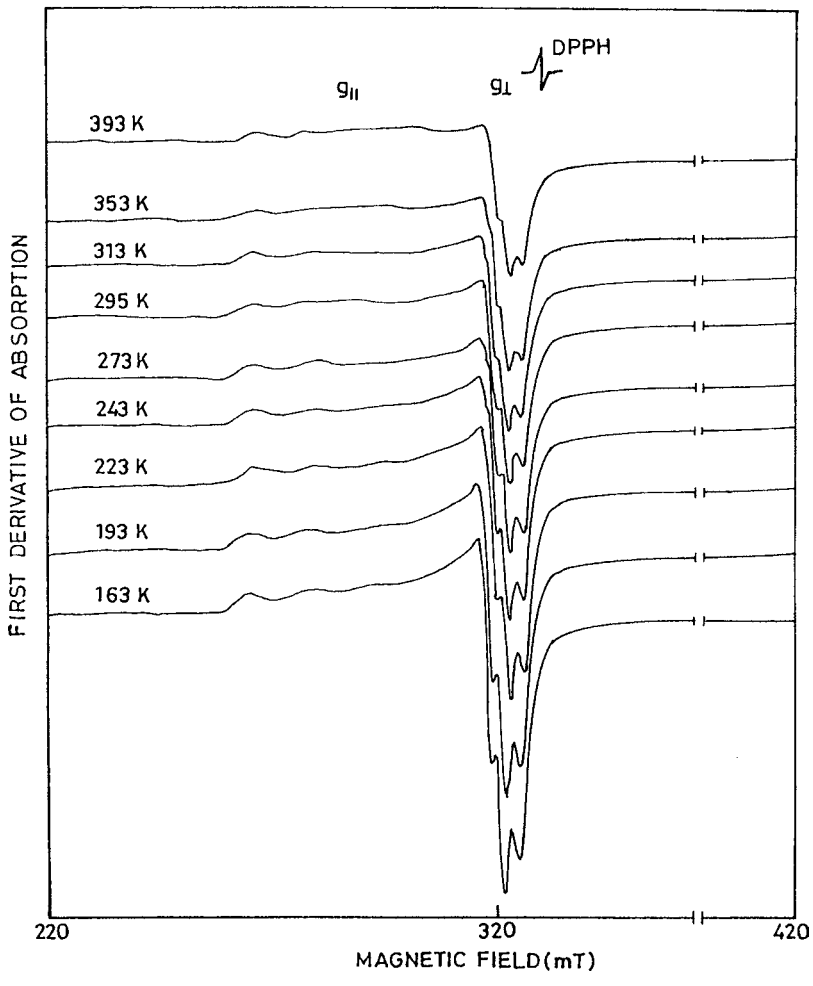

Figure 3 EPR spectra of 1 mol% of Cu^{2+} ions doped in sodium fluoride-sodium borate glass system at different temperatures.

3.5. Optical basicity

The optical basicity of an oxide glass will reflect the ability of glass to donate negative charge to the probe ion [18]. Duffy and Ingram [19] proposed that the optical basicity can be predicted from the composition of the glass and basicity moderating parameters of various cations present.

The theoretical values of the optical basicity (Λ_{th}) of the glasses can be calculated using the formula

$$\Lambda_{th} = \sum_{i=1}^{n} \frac{Z_i r_i}{|Z_0|\gamma_i} \tag{5a}$$

where 'n' is the number of cations present, 'Z_i' is the oxidation number of the ith cation, 'r_i' is the ratio of number of ith cation to the number of oxides present and 'γ_i' is the basicity moderating parameter of the ith cation. The basicity moderating parameter 'γ_i' can be calculated from the following equation

$$\gamma_i = 1.36(x_i - 0.26) \tag{5b}$$

where 'x_i' is Pauling electronegativity of the cation. The theoretical values of the optical basicity (Λ_{th}) of all the glass samples were calculated and are presented in Table I. It is observed that with the increase in copper content, the value of the optical basicity decreases.

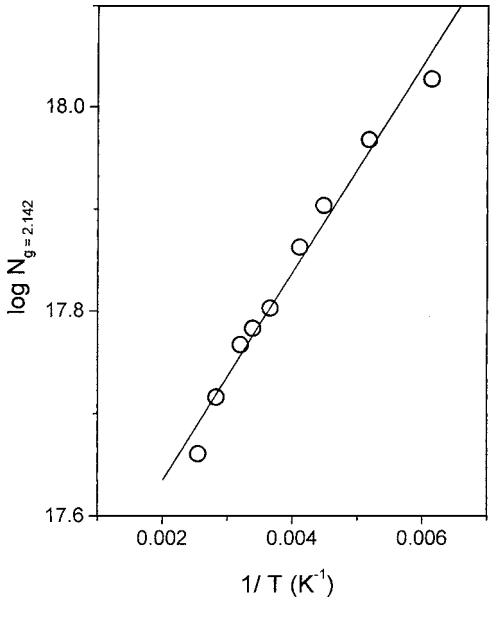

Figure 4 A plot of log N against $1/T$ for 1 mol% of Cu^{2+} ions containing sodium fluoride-sodium borate glass sample.

4. Discussion

4.1. EPR studies

For Cu^{2+} ions, a regular octahedral site may not exist because the cubic symmetry is disturbed by an electronic hole in the degenerate $d_{x^2-y^2}$ orbital that produces

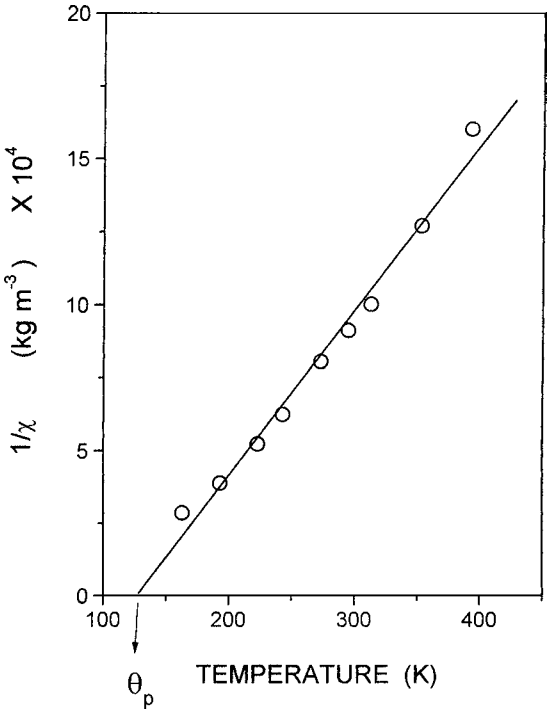

Figure 5 Plot of the reciprocal of susceptibility against T for 1 mol% of Cu^{2+} ions containing sodium fluoride-sodium borate glass sample.

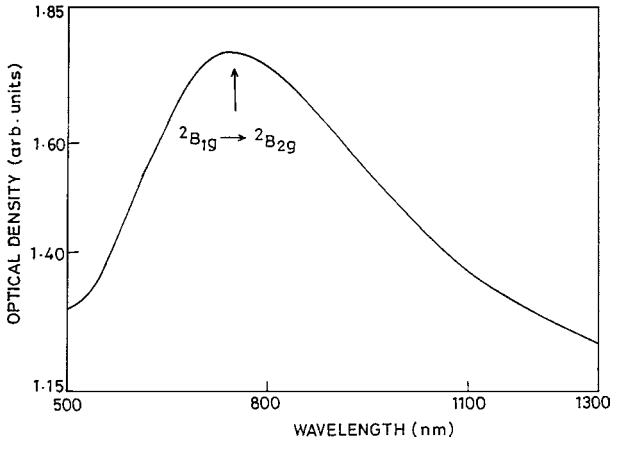

Figure 6 Optical absorption spectrum of sodium fluoride-sodium borate glass sample containing 0.5 mol% of Cu^{2+} ions at room temperature.

the tetragonal distortion. The EPR spectra of Cu^{2+} ions in the present glasses can be analysed by using an axial spin-Hamiltonian of the form

$$\mathcal{H} = \beta[g_\parallel B_z S_z + g_\perp (B_x S_x + B_y S_y)] + A_\parallel S_z I_z + A_\perp (S_x I_x + S_y I_y) \quad (6)$$

The symbols in the above equation have their usual meaning. The nuclear quadrupole and nuclear Zeeman interaction terms are ignored.

The solution of the spin-Hamiltonian gives the expression for the peak position of the principal 'g' and 'A' tensors as [20]

$$h\nu = g_\parallel \beta B + mA_\parallel + (15/4 - m^2)\frac{A_\perp^2}{2g_\parallel \beta B} \quad (7a)$$

$$h\nu = g_\perp \beta B + mA_\perp + (15/4 - m^2)\frac{A_\parallel^2 + A_\perp^2}{4g_\perp \beta B} \quad (7b)$$

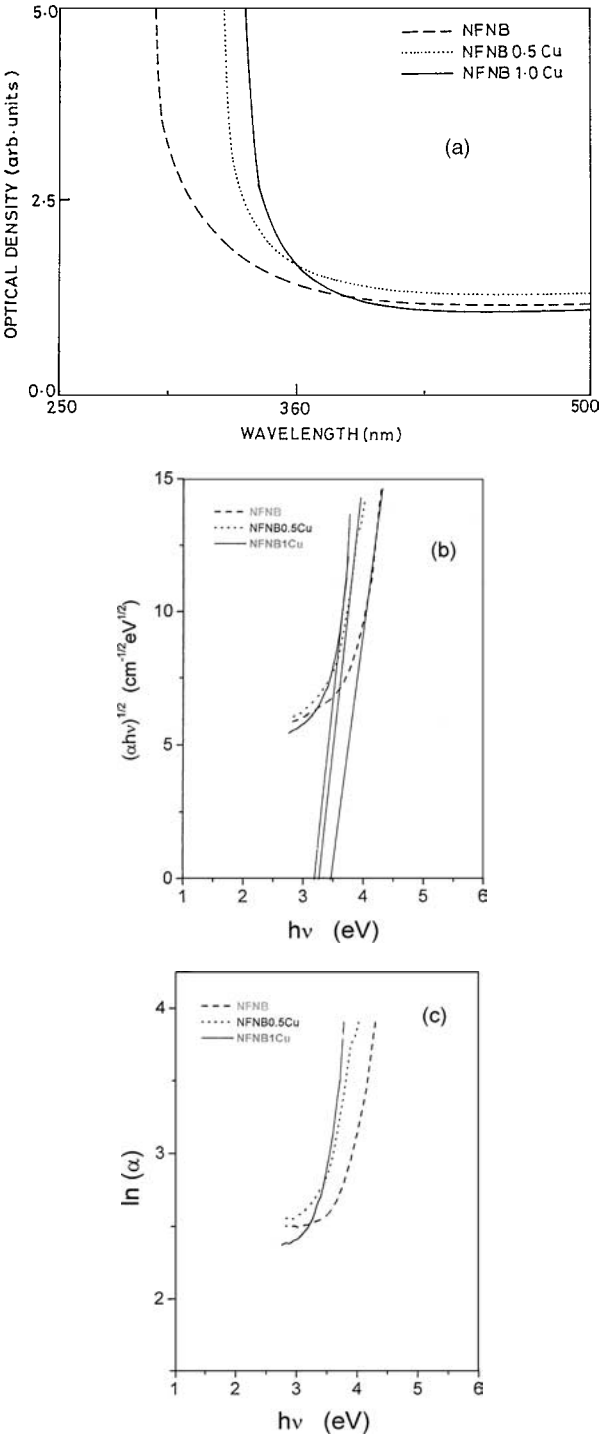

Figure 7 (a) Ultraviolet absorption edge, (b) A plot between $(\alpha h\nu)^{1/2}$ and $h\nu$ and (c) A plot between $\ln \alpha$ and $h\nu$ for NFNB, NFNB0.5Cu and NFNB1Cu glass samples.

for parallel and perpendicular peaks respectively, where 'm' is the nuclear magnetic quantum number of the copper nucleus with values 3/2, 1/2, −1/2 and −3/2 and 'ν' is the microwave frequency at resonance. Using Equation 7a and 7b, the spin-Hamiltonian parameters were evaluated and are presented in Table II. The calculated $g_\parallel$ and $g_\perp$ values are characteristic of Cu^2 ions coordinated by six ligands that form an octahedron elongated along the z-axis [11, 21–23]. As $g_\parallel > g_\perp > g_e$ (free electron g value), we consider that the ground state for paramagnetic electrons is $d_{x^2-y^2}$ orbital ($^2B_{1g}$ state); the Cu^{2+} ion being located in distorted octahedral sites

TABLE II Spin-Hamiltonian parameters and molecular orbital bonding coefficients for NFNB1Cu glass sample

Spin-Hamiltonian parameters		Molecular orbital bonding coefficients	
g-values	A values (10^{-4} cm^{-1})		
$g_\parallel = 2.313$	$A_\parallel = 153$	$\alpha^2 = 0.701$	$\Gamma_\pi = 18.49$
$g_\perp = 2.056$	$A_\perp = 26$	$\beta_1^2 = 0.897$	$\Gamma_\sigma = 65.14$

(D_{4h}) elongated along the Z-axis. We found that there is no significant change in spin-Hamiltonian parameters as the copper concentration is increased.

Fig. 1 shows asymmetric line, characteristic of Cu^{2+} ions in distorted octahedral sites. The spectrum preserves its asymmetric character within the entire concentration range proving a great structural stability of the matrix in accepting Cu^{2+} ions. Within the low concentration range ($0 \leq x \leq 2$ mol%), the spectrum shows well resolved hfs in both parallel and perpendicular components due to isolated Cu^{2+} ions. From Fig. 2, it is clear that as the concentration of Cu^{2+} ions is increased, the number of spins participating in resonance is increased monotonically and no cluster formation is observed till 2 mol% of Cu^{2+} ions. As the concentration of Cu^{2+} ions is increased beyond 2 mol%, the hfs resolution diminished. This is due to the individual lines broadening with the effect of increased dipolar interactions and ligand field fluctuations in the neighbourhood of the paramagnetic ion [23, 24].

Fig. 4 shows a plot of log N against $1/T$. It is observed that as the temperature is lowered, the number of spins increases and further we can observe a linear relationship between log N and $1/T$, a phenomenon that can be expected from the Boltzmann law. From the graph, the activation energy can be calculated. The activation energy thus calculated was found to be 3.457×10^{-21} J (0.0216 eV).

Fig. 5 shows a graph between reciprocal of susceptibility and absolute temperature. The graph is fitted to a straight line in accordance with the Curie's law. From the graph, the Curie constant (1.588×10^{-3}) and Curie temperature (119 K) have been evaluated. The Curie constant calculated in the present work is in good agreement with the measured value (1.61×10^{-3} emu/mol) reported for Cu^{2+} ions in borate glasses [25].

4.2. Optical absorption spectrum

The observed single broad band centred at 13280 cm^{-1} has been assigned to $^2B_{1g} \rightarrow {}^2B_{2g}$ transition of Cu^{2+} ions in distorted octahedral sites. A band corresponding to $^2B_{1g} \rightarrow {}^2E_g$ transition at higher energy side could not be observed. The Cu^{2+} lacks cubic symmetry and this cubic symmetry is disturbed by electronic hole in the degenerate orbital which produces the tetragonal distortion. The Jahn-Teller theorem requires that any non-linear system with a degenerate ground state must distort in order to remove the degeneracy. Then two structures are to be expected. One elongated and the other compressed structure. Experimental data show that the cupric ion generally exists in solutions, solids and glasses in octahedral symmetry with a strong tetragonal distortion [12, 26–28]. According to the present EPR studies, Cu^{2+} ions in NFNB glasses present in octahedral symmetry with elongated tetragonal distortion.

4.3. Molecular orbital coefficients

The EPR and optical absorption data can be correlated to evaluate the bonding coefficients as follows [29]

$$g_\parallel = 2.0023\left[1 - \frac{4\lambda\alpha^2\beta_1^2}{E_1}\right] \tag{8a}$$

$$g_\perp = 2.0023\left[1 - \frac{\lambda\alpha^2\beta^2}{E_2}\right] \tag{8b}$$

E_1 and E_2 are the energies corresponding to the transitions $^2B_{1g} \rightarrow {}^2B_{2g}$ and $^2B_{1g} \rightarrow {}^2E_g$ respectively and 'λ' is the spin orbit coupling constant (-828 cm^{-1}) [30]. The parameters α^2 and β_1^2 represent the contribution of 3d atomic orbitals of the cupric ion to the B_{1g} and B_{2g} anti bonding orbitals respectively. The bonding coefficients α^2, β_1^2 and β^2(=1.00) characterize respectively, the in-plane σ bonding, in-plane π bonding and out of plane π bonding of the Cu^{2+} ligand bond in the glasses. The values of these parameters lie between 0.5 and 1.0, the limits of pure covalent and pure ionic bodings [12]. The value of β^2 may be expected to lie sufficiently close to unity so as to be indistinguishable from unity in the bonding coefficient calculations [31]. The expression α^2 given in Equation 8a is the bonding coefficient due to the covalancy of the σ bonds with the equatorial ligands which measures the electron density delocalized on the ligand ions and β_1^2 accounts for covalency of π-anti bonding between ligands and the excited $^2B_{2g}$ state.

The bonding coefficient α^2 (in-plane σ bonding) can be calculated from the EPR data using the following expression given by Kuska *et al.* [32].

$$\alpha^2 = \frac{7}{4}\left[\frac{A_\parallel}{P} - \frac{A}{P} - \frac{2}{3}g_\parallel - \frac{5}{21}g_\perp + \frac{6}{7}\right] \tag{9}$$

where $P = 0.036$ cm^{-1} and $A = (1/3A_\parallel + 2/3A_\perp)$. The α^2 value calculated from the above equation was used in Equation 8 to evaluate β_1^2.

From the Equation 8a and b, it can be seen that to determine Cu^{2+} bonding coefficients, one needs in addition to the EPR parameters the energy positions of the absorption band of Cu^{2+} which indicates the values of E_1 and E_2. Since the authors have observed only one absorption band corresponding to the transitions $^2B_{1g} \rightarrow {}^2B_{2g}$, the position of second band can be estimated by the approximation [12].

$$E\left(^2B_{1g} \rightarrow {}^2E_g\right) = \frac{2k^2\lambda}{2.0023 - g_\perp} \tag{10}$$

where k^2 is the orbital reduction factor ($k^2 = 0.77$). The calculated bonding coefficient values are given in Table II.

If $\alpha^2 = 1$, the bond would be completely ionic. If the overlapping integral were vanishingly small and $\alpha^2 = 0.5$, the bond could be completely covalent. However, because the overlapping integral is sizeable, we cannot speak strictly of covalent versus ionic bonds but we can say that the smaller the value of α^2, the greater the covalent nature of the bond. The cupric ion is a network modifier and $Na_2B_4O_7$ is a network former. The β_1^2 reflects the competition between the cupric ion and its neighbouring former cations for attracting the lone pairs of the intervening oxygen ions. The value of β_1^2 depends strongly on network modifier. In the present work, the values of the calculated parameters α^2 and β_1^2 indicate that the in-plane σ bonding is covalent where as in-plane π bonding is significantly ionic in nature.

The normalised covalency of the Cu(II)-O in-plane bondings of σ and π symmetry are expressed [11] in terms of bonding coefficients α^2 and β_1^2 as follows

$$\Gamma_\sigma = \frac{200(1-S)(1-\alpha^2)}{1-2S}\% \qquad (11a)$$

$$\Gamma_\Pi = 200\left(1-\beta_1^2\right)\% \qquad (11b)$$

where 'S' is the overlap integral ($S_{\text{oxygen}} = 0.076$). The normalised covalency values of the Cu(II)-O of in-plane bonding of π symmetry (Γ_Π) thus calculated are given in Table II.

4.4. Optical energy gap and Urbach energy

The values of the optical energy gap and Urbach energy calculated in the present work for different glasses are presented in Table III. The values obtained in the present work are of the same order for those of copper tellurium oxide [15] and borate glasses [33] reported in literature. The optical band gap energy for the NFNB1Cu glass sample (3.193 eV) is far greater than the activation energy (0.0216 eV) calculated from EPR spectra at different temperatures (Fig. 4). Hassan and Hogarth [15] also observed a similar phenomenon where they calculated the activation energy from the DC conductivity measurements at different temperatures. This can be explained by suggesting that the activation energy is not across the whole gap but is possibly from one or more trapping levels to the conduction band or from bonding states to a trapping level.

The values of E_{opt} are found to decrease as CuO content increases because CuO introduces additional defect states (e.g., Colour centres) in the glass matrix [34]. The density of localised states, $N(E)$, was found to be proportional to the concentration of these defects [35] and consequently to CuO content. Increasing CuO content may cause the localised states of the colour centres to overlap and extend in the mobility gap [36]. This overlap may give us evidence for decreasing E_{opt} when CuO content is increased in the glass matrix.

From the values of the widths of the tails of the localised states (ΔE) within the optical band gap for the present glasses, it can be observed that the least Urbach energy (0.387 eV) is observed for undoped (NFNB) glass sample. This suggests that defects are minimum in undoped glass sample. The increase in Urbach energy with Cu^{2+} concentration can be considered as due to increased defects [37].

TABLE III Optical band gap and Urbach energies for copper doped in sodium fluoride–sodium borate glass samples

Glass sample	Optical energy gap (E_{opt}) (eV)	Urbach energy (ΔE) (eV)
NFNB	3.45	0.387
NFNB0.5Cu	3.26	0.418
NFNB1Cu	3.19	0.510

5. Conclusions

1. From the EPR and optical spectra of Cu^{2+} ions in sodium fluoride-sodium borate glasses, it is found that the copper ions occupied octahedral sites with tetragonal distortion.

2. The EPR spectra of copper ions at different temperatures show a linear dependence between log N and $1/T$. The activation energy is calculated and is found to be 0.0216 eV.

3. From the EPR data, the susceptibilities are calculated for NFNB 1Cu sample at various temperatures. The linear dependence between $1/\chi$ and T is used to calculate the Curie constant and found to be in good agreement with the value reported in literature for copper ions in glasses.

4. The optical absorption spectra of these samples show single broad band due to Cu^{2+} ions in distorted octahedral sites.

5. The optical energy gap and the Urbach energies are found to vary with CuO content which is assigned to the increase in defect concentration with increase in CuO content.

6. By correlating the EPR and optical data, the molecular orbital coefficients α^2 and β_1^2 are evaluated. The values suggest that the in-plane σ bonding is moderately covalent and the in-plane π bonding is significantly ionic in nature.

Acknowledgements

One of the authors (JLR) is thankful to University Grants Commission (New Delhi) for financial support.

References

1. H. NASU, T. UCHIGAKI, K. KAMIYA, H. KANBORA and K. KUBODERA, *Jpn. J. Appl. Phys.* **31** (1992) 3899.
2. R. GOPALAKRISHNAN, in "Solid State Materials," edited by S. Radhakrishna and A. Daued (Springer-Verlag, Berlin, 1991) p. 1220.
3. A. J. BRUCE and J. A. DUFFY, *Phys. Chem. Glasses* **23**(2) (1982) 53.
4. C. C. HUNTER and M. D. INGRAM, *Solid State Ionics* **14** (1984) 31.
5. Y. WANG, A. OSAKA, Y. MIURA and K. TAKAHASHI, *J. Mater. Res* **2** (1987) 606.
6. J. E. SHELBY and R. L. ORTOLANO, *Phys. Chem. Glasses* **31**(1) (1990) 25.
7. H. KAWAZOE, H. HOSONO and T. KANAZAWA, *J. Non-Cryst. Solids* **29** (1978) 173.
8. A. K. BANDYOPADHYAY, *J. Mater. Sci.* **15** (1980) 1605.

9. A. MURALI and J. LAKSHMANA RAO, *J. Phys. Condens. Matter.* **11** (1999) 7921.
10. J. A. WEIL, J. R. BOLTAN and J. E. WERTZ, in "Electron Paramagnetic Resonance—Elementary Theory and Practical Applications" (Wiley, New York, 1994) p. 498.
11. H. KAWAZOE, H. HOSONO and T. KANAZAWA, *J. Non-Cryst. Solids* **33** (1979) 103.
12. A. KLONKOWSKI, *Phys. Chem. Glasses* **24** (1983) 116.
13. R. P. SRIKANTH CHAKRADHAR, A. MURALI and J. LAKSHMANA RAO, *J. Alloys Compds.* **265** (1998) 29.
14. G. RAMADEVUDU, MD. SHAREEFUDDIN, N. SUNITHA BAI, M. LAKSHMIPATHI RAO and M. NARASIMHA CHARY, *J. Non-Cryst. Solids* **278** (2000) 205.
15. M. A. HASSAN and C. A. HOGARTH, *J. Mater. Sci.* **23** (1988) 2500.
16. E. A. DAVIS and N. F. MOTT, *Phil. Mag.* **22** (1970) 903.
17. G. FUXI, in "Optical and Spectroscopic Properties of Glasses" (Springer, Berlin, 1992) p. 62.
18. A. J. EASTEAL and A. T. MARCOM, *J. Non- Cryst. Solids* **34** (1979) 29.
19. J. A. DUFFY and M. D. INGRAM, *J. Inorg. Nucl. Chem.* **37** (1975) 1203.
20. B. BLEANEY, K. D. BOWERS and M. H. L. PRYCE, *Proc. Roy. Soc.* A **228** (1955) 147.
21. L. D. BOGOMOLOVA, YU. G. TEPLIAKOV and F. CACCAVALE, *J. Non-Cryst. Solids* **194** (1996) 291.
22. T. TAOUFIK, M. HADDAD, A. NADIRI, R. BROCHU and R. BERGER, *J. Phys. Chem. Solids* **60** (1999) 701.
23. I. ARDELEAN, M. PETEANU, R. CICEO-LUCACEL and I. BRATU, *J. Mater. Sci. Mater. Electron.* **11** (2000) 11.
24. F. CIORCAS, S. K. MENDIRATTA, I. ARDELEAN and M. A. VALENTE, *Eur. Phys. J.* (B) **20** (2001) 235.
25. I. ARDELEAN, O. COZAR, S. FILIP, V. POP and CENAN, *Solid State Commun.* **100** (1996) 609.
26. T. BATES, in "Modern Aspects of the Vitreous State," edited by J. D. Mackenzie (Butterworths, London, 2, 1962) p. 195.
27. R. HARANI, C. A. HOGARTH and K. A. K. LOTT, *J. Mater. Sci.* **19** (1984) 1420.
28. R. R. KUMAR, A. K. BHATNAGAR and B. C. V. REDDY, *Solid State Commun.* **114** (2000) 493.
29. D. KIVELSON and R. NEIMAN, *J. Chem. Phys.* **35** (1961) 145.
30. F. M. MABBS and D. J. MACHIN, in "Magnetism and Transition Metal Complexes" (Chapman and Hall, London, 1973) p. 154.
31. H. IMAGAWA, *Phys. Stat. Solidi.* **30** (1968) 469.
32. H. A. KUSKA, M. T. ROGERS and R. E. DURLLINGER, *J. Phys. Chem.* **71** (1967) 109.
33. A. I. SABRY and M. M. EL-SAMANOUDY, *J. Mater. Sci.* **30** (1995) 3930.
34. C. K. JORGENSEN, *Acta Chem. Scand.* **11** (1957) 73.
35. N. F. MOTT, *Philos. Mag.* **24** (1970) 903.
36. R. MURI, L. SCHIAVULLI, N. PINTO and T. LIGONZE, *J. Non-Cryst. Solids* **139** (1992) 60.
37. M. VITHAL, P. NACHIMUTHU, T. BANU and R. JAGANNATHAN, *J. Appl. Phys.* **81** (1997) 7922.

Received 16 December 2002
and accepted 18 August 2003